*34th EPS Conference on Plasma Phys. Warsaw, 2 - 6 July 2007 ECA Vol.**31F**, P-2.049 (2007)*

Study of Z-dependence of impurity transport at JET

C. Giroud[1], C. Angioni[2], L. Carraro[3], I.H. Coffey[4], J. Hobirk[2], M.E. Puiatti[3], M. Valisa[3], A.D. Whiteford[5], P. Belo[6], T.M. Biewer[7], M. Brix[1], R. Buttery[1], E. Joffrin[8], L. Lauro Taroni[3], K. Lawson[1], P. Mantica[9], A. Meigs[1], V. Naulin[10], M.G. O'Mullane[5], K-D. Zastrow[1] and the JET-EFDA Contributors[*].

[1]*EURATOM-UKAEA Association, Culham Science Centre, Abingdon, OX14 3DB UK.*
[2]*Max-Planck-Institut fur Plasmaphysik, EURATOM Association, D-85748 Garching, Germany.*
[3]*Consorzio RFX Associazione EURATOM-ENEA sulla Fusione, I-35127 Padova, Italy.*
[4]*Department of Physics, Queens University, Belfast, BT7 1NN, U.K.*
[5]*Department of Physics, University of Strahclyde, Glasgow, G4 ONG, U.K.*
[6]*EURATOM/IST Fusion Association, Centro de Fusao Nuclear, Av. Rovisco Pais 1049.001 Lisbon, Portugal.*
[7]*Oak Ridge National Laboratory,Oak Ridge, TN 37831, USA*
[8]*CEA-Cadarache,Association Euratom-CEA, 13108 St Paul-lez-Durance, France.*
[9]*Istituo di Fisica del Plasma, Associazione Euratom-ENEA-CNR, Milano, Italy.*
[10]*Risø NationalLaboratory, Technical University of Denmark, OPL-128, 4000 Roskilde, Denmark.*
[*]*See Appendix of M.L. Watkins et al, Fusion Energy 2006 (Proc 21st Int Conf. Chengdu, 2006) IAEA.*

The development of an ITER scenario will be an optimisation between confinement, stability and pollution by impurities. It will have to take into account the transport of He, with a charge of 2, product of the D-T reaction but also the transport of impurities originating from the plasma edge resulting from the sputtering of the wall and divertor material, i.e. Be (Z=4), C (Z=6) and W (Z=74). The reduction of the divertor power load will also require seeding impurity such as Ar (Z=18). Clearly, the understanding of the Z dependence of impurity transport is, if not necessary, a beneficial tool for the optimisation of ITER scenarios.

In addition, the study of the Z dependence of impurity transport gives insight into mechanisms at play, in particular how micro-instabilities drive particle transport, and highlights the regions influenced by neoclassical transport. Initial results on the Z dependence of impurity transport in H-mode discharge were reported in [1] and compared with theoretical predictions.

During the 2006-2007 campaign, experiments have specifically focused on clarifying the Z dependence of trace impurity transport in various plasma conditions. L-mode, H-mode discharges have been probed. The aim is to characterise the variation in the Z dependence of impurity transport across the plasma radius, and also to document for which plasma conditions an effect of the neoclassical transport is observed.

Methodology

The study of the Z dependence of impurity transport in various plasma conditions is performed by injecting three impurities Ne, Ar and Ni with respective Z of 10, 18 and 28 in the same discharge at similar time via a short gas puff for Ne and Ar and a laser ablation for Ni. The density profile of Ne^{10+} and Ar^{18+} are tracked simultaneously via the recently upgraded charge-exchange recombination spectroscopy diagnostic [2]. These improvements include an increased time resolution from 50 to 10ms and a doubling of the plasma viewing coverage. The density of the fully stripped C, an intrinsic impurity is also measured with the charge-exchange diagnostic. The transport of Ni is inferred from the soft X-ray signals. The transport coefficients of these impurities are determined by reproducing the measured densities, soft x-ray signals and vacuum ultra-violet line intensities within the impurity transport code UTC-SANCO [3]. A linear relationship is assumed between impurity flux and density, i.e. $\Gamma_z=-D_z\ \partial n_Z/\partial r + V_z\ n_z$, with a positive velocity is outward. Further details on the method used to determine the transport coefficients and an estimate of their uncertainty are reported in the [4]. Pseudo steady-state profiles can be

Table 1: Parameters of studied discharges

pulse	type	Ip (MA)	Bt (T)	NBI (MW)	ICRH (MW)	q95
67730	L-mode	1.8	3	4.2	0	5.7
67732	L-mode	1.5	2.6	4.2	0	5.7
67680	L-mode	2	3.4	5.6	0	5.5
67679	L-mode	2	3.4	7.1	0	5.5
66134	H-mode	1.5	3	8.3	1.6	6.9
69808	H-mode	1.8	3.2	11.5	0	6
69809	H-mode	1.8	3.2	14.2	0	6
69812	H-mode	1.8	3.2	12.7	2.9	5.9
69813	H-mode	1.8	3.2	11.7	3.1	6.1

calculated within UTC-SANCO with the determined transport coefficients assuming a constant edge source. In this paper, the steady-state profiles have been normalised to the value at r/a~0.75.

Comparison L-mode and H-mode discharge

The dependence of the transport of impurity with the charge was investigated in L-mode and type III H-mode with plasma currents varying from 1.5 to 2MA and magnetic field varying from 2.6 to 3.4 T. Details characteristics are listed in Table 1. The transport of impurity was probed for the duration of trace impurities presence in the discharge as shown in Figure 1 for one of the H-mode discharge studied. The temperature profiles, electron density profile are shown in Figure 2 together with the safety factor.

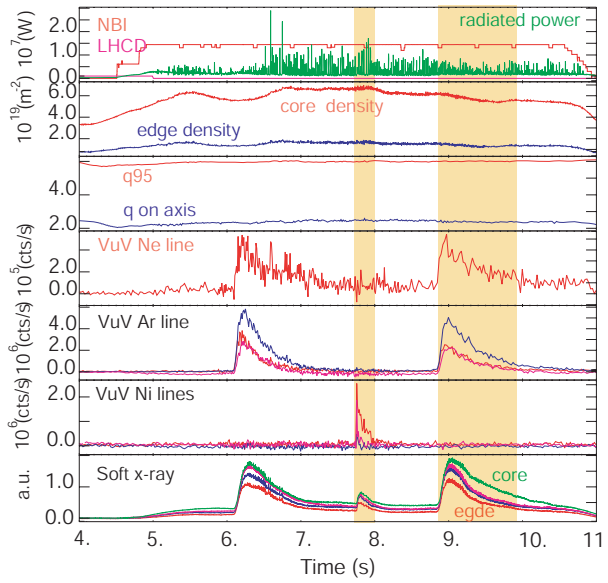

Figure 1: General plasma parameters for shot 69809 with spectroscopic measuremens indicating duration of trace impurities presence in discharge.

The determination of transport coefficients for the considered L-mode discharges was not as straightforward as could have been expected without the presence of ELMs or MHD modes. Data quality did not allow the analysis for all impurities in each discharge. However, the transport coefficients have been determined for a range of similar L-mode plasmas for Ne, Ar and Ni. An estimate of the error on H-mode discharges has been determined with method presented in [4]. Full error propagation is outside the scope of this paper but is planned for future work.

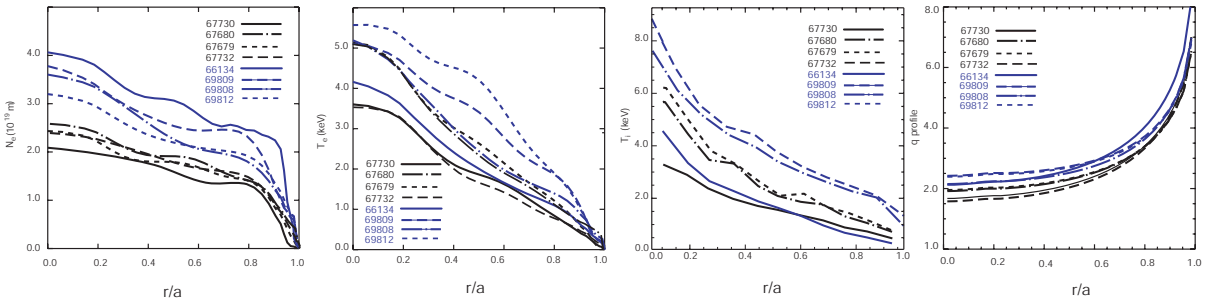

Figure 2: Electron density, electron temperature, ion temperature profiles of studied discharges and safety factor profiles as determined from EFIT.

The transport coefficients have been determined for Ne, Ar and Ni and are shown together with their neoclassical values in the core region and at mid-radius in Figure 3. The peaking of the impurity profile shown in Figure 3 has been determined from the gradients in the steady-state profile, shown in Figure 4, over the region r/a from 0. to 0.3 for the core and from 0.5 to 0.6 for the mid-radius values. For both L and H-mode discharges, the diffusion of Ne, Ar and Ni at mid-radius is ~2-4$m^2.s^{-1}$, two orders of magnitude above its neoclassical levels, whereas it is reduced in the core to a value ~0.06-0.6$m^2.s^{-1}$ roughly an order of magnitude above its neoclassical level. It should be noted that the region of reduced diffusion in the studied L-mode discharges seem to be closely related to the position of the q=2 surface. The convection coefficients shown in Figure 3 are of a similar order with the neoclassical values. For both L and H-mode discharges, the peaking factor in the core shows a clear Z dependence over the studied discharges and varies from ~0.5 m^{-1} to 4m^{-1} from C to Ni. (The error in the determination of Ni peaking in the core is higher due to the use of the line integrated soft x-ray measurement for the determination of the transport coefficients). The peaking of impurity profile in the core region is influenced by neoclassical transport.

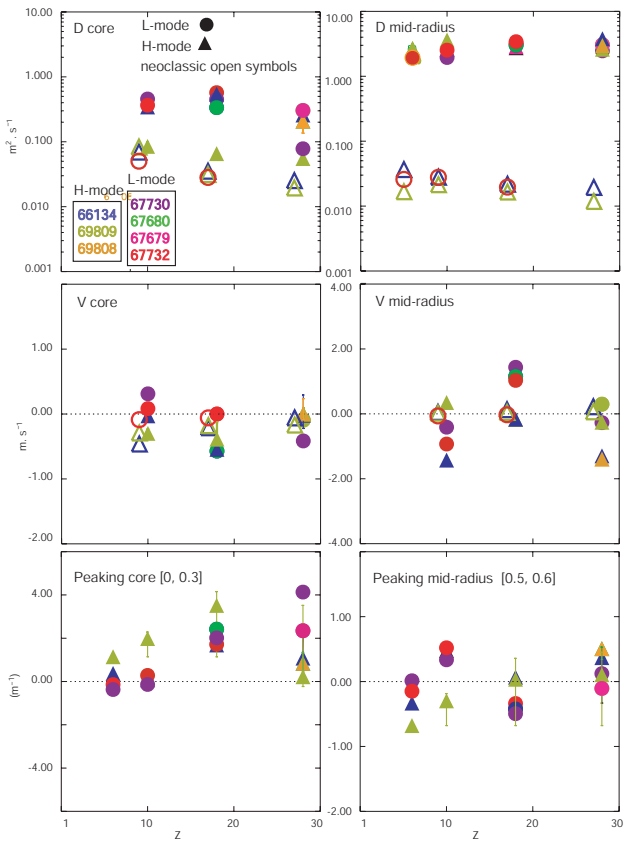

Figure 3: Diffusion, convection in the core and at mid-radius determined for L and H-mode discharges against neoclassical values in open symbols. The peaking factor has been determined from the gradient s of the steady-state profiles shown in Figure 4.

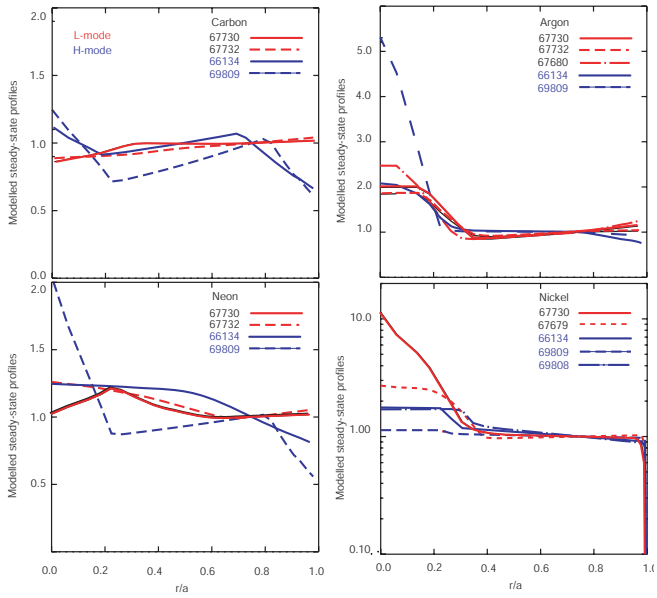

Figure 4: Steady-state profiles for studied L and H-mode discharges calculated from determined transport coefficients assuming a constant edge source.

In the region between r/a of 0.5 and 0.6, the peaking is smaller and varies at the maximum from -1 to 0.5 m^{-1} from C to Ni although variations are observed between discharges. These values are much lower than expected by neoclassical transport. No clear difference is observed in the transport of impurity in the core or at mid-radius between L and H-mode discharges.

Effect of ICRH on core transport

Observations were made at JET that the convection coefficient of Ni changes from inward to outward with the application of ion cyclotron resonance frequency (ICRF) heating [5]. Dedicated experiments have been performed at JET to study the effect of ICRF heating by probing the transport of trace Ne, Ar and Ni in H-mode discharges with no ICRF and with 3MW of ICRF heating. The transport of Ni in some of these discharges is also reported in [6] but was analysed with different tools and method.

It should be pointed out that in some of the discharges studied (69809, 69812 and 69813) a 2/1 NTM is observed at r/a~ 0.2 with an island width less than 10cm, however the time evolution and profile of Ne^{10+} and Ar^{18+} density seems unaffected. In addition, the determined transport coefficients for Ni are similar in consecutive discharges with and without the mode (see figure 3 for discharge 69808 and 69809). The 2/1 NTM does not seem to affect the transport of impurity significantly probably due to a small island width. In any case, the amplitude of the mode in the discharges of interest is similar which justifies the comparison of transport coefficients.

The change of Ni profile following the application of ICRF heating is confirmed as shown in Figure 5. The steady-state profiles of Ni change from peaked in the core to hollow with 3MW of ICRF heating. In addition, the steady-state profiles of C, Ne and Ar also changed from peaked in the core to hollow. But, it appears from the C, Ne and Ar steady-state profiles that this effect is localised in the core within a region inside r/a~0.25. It is possible that this effect is also due to a change in core transport but appears wider for Ni due to the use of line integrated measurements.

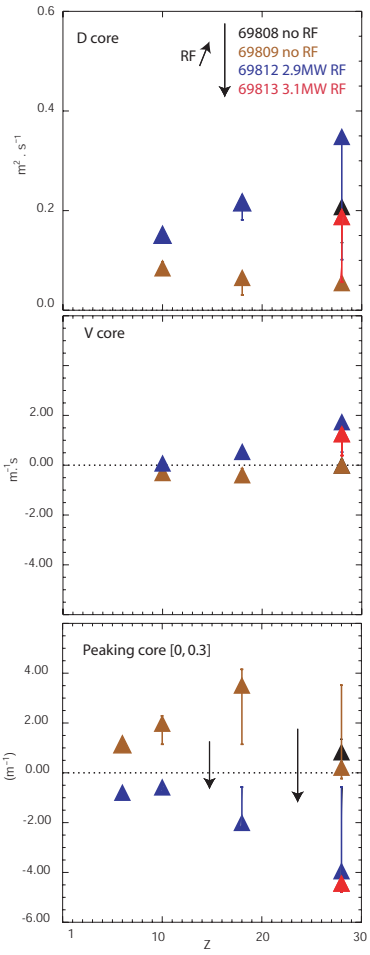

Figure 6: Diffusion, convection and peaking factor in the core region for discharge with varied ICRF heating power.

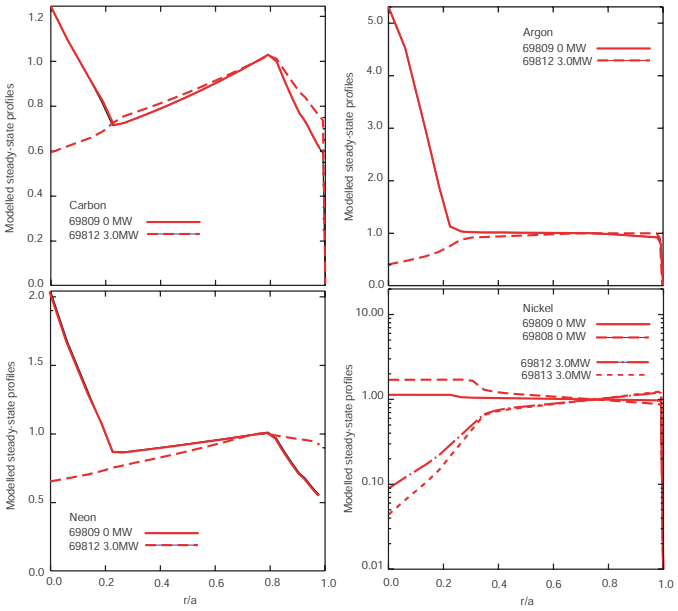

Figure 5: Steady-state profiles of C, Ne, Ar and Ni for discharge varied ICRF heating power as indicated on the legend.

The change of transport following the application of ICRF heating is linked to a change of convection from inward to outward for Ne, Ar and Ni, as can be seen in Figure 6. The core diffusion does not change significantly. In addition, it is observed that the change of peaking in core following ICRF heating is dependent on the charge as shown in Figure 6. The ICRF heating is modifying the core peaking of Ni more than Ne or C.

Summary

First results of the database constituted for the study of the Z dependence of impurity transport have been reported. L and H-mode discharges have been studied. No clear difference is observed between L and H-mode in the transport coefficients in the core and at mid-radius. A dependence of the impurity peaking with Z is observed in the core for both L and H-mode and varies between -0.5 to a maximum of 4 m^{-1} from C to Ni for the discharges studied. In the region between 0.5 and 0.6, the peaking of impurity profile shows a weaker dependence in Z from roughly a maximum of -0.5 to 0.5 m^{-1} from C to Ni for the studied discharges.

The observation of the pinch reversal from inward to outward for Ni [5] was confirmed following the application of ICRF heating power. This pinch reversal is also observed for C, Ne and Ar but is restricted to a change of transport in the plasma core within r/a less 0.25. The change of peaking following the application of ICRF is dependent on the charge of the impurity and is stronger for Ni than for C.

[1] C. Giroud *et al* EX/8.3 IAEA Chengdu, China (2006)
[2] C.R. Negus C.R. , C.Giroud, A. G. Meigs *et al*, Rev. Sci. Instrum. 77, 10F102 (2006).
[3] A.D. Whiteford, PhD thesis University of Strathclyde, Glasgow, (2004)..
[4] C. Giroud, *et al* Nucl. Fus, 47 , 313-330, (2007)
[5] M.E. Puaitti *et al*., Phys. Plasma 13, 042501, (2006)[6] L. Carraro at this conference
[6] L. Carraro *et al* this conference.

This work was partly supported by the UK Engineering and Physical Sciences Research Council and by the European Communities under the contract of Association between EURATOM and UKAEA. The views and opinions expressed herein do not necessarily reflect those of the European Commission. This work was partly conducted under the European Fusion Development Agreement.